ChemElectroChem

Research Article
doi.org/10.1002/celc.202300004

Chemistry Europe
European Chemical Societies Publishing

www.chemelectrochem.org

Special Collection

# Voltammetric Sensor Based on Waste-Derived Carbon Nanodots for Enhanced Detection of Nitrobenzene

Viviana Bressi,[a, b] Isabella Chiarotto,*[c] Angelo Ferlazzo,[a] Consuelo Celesti,[a, d] Cinzia Michenzi,[c] Thomas Len,[b] Daniela Iannazzo,[a] Giovanni Neri,[a] and Claudia Espro*[a]

Carbon dots (CDs) samples were synthesized from orange peel waste (OPW) via a simple and eco-friendly hydrothermal carbonization (HTC) and electrochemical (EC) bottom-up synthesis integrated approach. The comprehensive chemical-physical characterization of CDs samples, carried out by various techniques such as TEM, EDX, XRD, FT-IR, underlined their morphological and microstructural features. The CDs exhibited attractive electrochemical properties, and thus an electrochemical sensor by modifying a screen printed carbon electrode (CDs/SPCE) for the detection of nitrobenzene (NB) in water was developed. Electroanalytical performances of CDs/SPCE sensor using differential pulse voltammetry (DPV) demonstrated its high sensitivity (9.36 $\mu A\,\mu M^{-1}\,cm^{-2}$) towards NB in a wide linear dynamic range (0.1–2000 μM) and a low limit of detection (LOD = 13 nM). The electrochemical sensor also shown high selectivity, long-term stability, and repeatability. This paper might open the way to a new synergistic HTC-EC approach for the synthesis of CDs from waste biomass material and their advanced application in highly efficient electrochemical sensors.

## Introduction

The orange juice industry produces large amounts of orange peel waste (OPW) each year, which requires proper management, taking into account the high biodegradability of orange processing waste, which causes rapid fermentation.[1,2] Both from the economical and eco-friendly points of point of view, wastes of industrial and agricultural processes are very attractive for their low cost and to chance to recover the manufactured side-products and reconvert them to useful materials. Therefore, the production of new carbon nanostructures from these wastes is highly demanding and covers a wide range of application fields.[3] Natural raw materials such as biomass and plant wastes are the most interesting feedstock for the synthesis of carbonaceous nanomaterials due to their high availability, environmental compatibility, and affinity with Green Chemistry principles.[4–6] Carbon dots (CDs), a new class of carbon-based zero-dimensional materials, typically less than ≈10 nm in diameter, exhibiting excellent photostability and biocompatibility, low cytotoxicity, fluorescence, and ease of surface modification, have attracted much attention due to their interesting properties, leading to diverse applications in catalysis, bio-imaging, drug delivery, and so on. In recent years, hydrothermal carbonization (HTC) has become the cornerstone of the synthesis of nanomaterials from natural sources thanks to the mild reaction conditions and the large amount of products obtained.[7–9] The HTC of the OPW, provides solid (hydro-char), liquid, and non-condensable gaseous products.[10,11] However, the aqueous phases generated from HTC treatment of OPW are generally considered as by-products, and there are few studies addressing their use as a resource for value-added chemicals.[12]

The electrochemical (EC) approach represents an efficient and easily repeatable method for the preparation of high-quality CDs,[13] starting from the liquid fraction obtained via the hydrothermal treatment. EC methods offer the advantages of mild reaction conditions, high yields, and purity, simple instrumentation, and cost containment for mass production. Furthermore, the popularity of electricity as a reagent is enhanced by the efficient conversion of wet agro-industrial biomass through a circular chemistry approach.[14,15]

The excellent properties of CDs nanomaterials allow researchers to develop new electrochemical sensing strategies with enhancing sensitivity, selectivity, and stability.[16] Nitro-

[a] Dr. V. Bressi, Dr. A. Ferlazzo, Dr. C. Celesti, Prof. D. Iannazzo, Prof. G. Neri, Prof. C. Espro
Department of Engineering
University of Messina
Contrada di Dio–Vill. S. Agata, I-98166 Messina (Italy)
E-mail: claudia.espro@unime.it
Homepage: https://archivio.unime.it/it/persona/claudia-espro
[b] Dr. V. Bressi, Dr. T. Len
Department of Organic Chemistry
University of Córdoba
Campus de Rabanales, Marie Curie (C-3), Ctra Nnal IV–A, Km 396 Cordoba (Spain)
[c] Prof. I. Chiarotto, Dr. C. Michenzi
Department of Basic and Applied Sciences for Engineering (SBAI)
Sapienza University of Rome
Via Castro Laurenziano, 7, 00161 Rome (Italy)
E-mail: isabella.chiarotto@uniroma1.it
Homepage: https://corsidilaurea.uniroma1.it/it/users/isabellachiarottouniroma1it
[d] Dr. C. Celesti
Department of Clinical and Experimental Medicine
University of Messina
Via Consolare Valeria, 98125 Messina, (Italy)

Supporting information for this article is available on the WWW under https://doi.org/10.1002/celc.202300004

An invited contribution to a Special Collection dedicated to Giornate dell'Elettrochimica Italiana 2022 (GEI2022)

benzene (NB), a common substance in the benzene series, is a highly toxic pollutant that is difficult to break down under natural conditions and can cause serious contamination of drinking water and irrigation systems. NB and its several derivatives are widely used in industry, especially in the manufacture of pesticides,[17] rubber,[18] textile dyes,[19] explosives[20] and precursors for the synthesis of pharmaceuticals and organic compounds.[21] Environmental monitoring of NB is of great importance, as it is a compound considered toxic and hazardous. For this reason, several methods have been used in recent years to detect NB, but most of them involve harmful chemicals and expensive equipment that complicate the monitoring processes.[22]

The electrochemical detection method can be considered the most powerful approach due to its portable equipment, high sensitivity, selectivity, speed, and ease of installation, which opens a wide range of possibilities for its practical application for monitoring in situ and multi-element detection.[23,24] In recent years, screen-printed carbon electrodes (SPCEs), which can be inexpensively, easily, and rapidly produced in bulk using thick-film technology, have been extensively used to develop innovative electrochemical sensing platforms and improve their performance.[25,26] In the present work, the OPW was converted into CDs by a simple and environmentally friendly HTC and EC bottom-up synthesis in a synergistic approach. Moreover, carbonaceous nanomaterials can be also obtained from the hydrochar produced during HTC, instead in this work, they were obtained from the aqueous solution of the hydrothermal process, in the combined approaches (HTC-EC) to synthesize nanomaterials from waste. In fact, both the approaches HTC and EC are effective in manufacturing carbon dots of different sizes and characteristics. However, bottom-up methods generally led to the production of CDs with well-defined sizes and shapes, so the bottom-up approach should be the preferred route for preparing carbon nanoparticles for biosensing application.[15] Up to now, it is the first time that an EC procedure on waste materials to produce CDs is presented, and the first comprehensive work on the valorisation of OPW to produce value-added products through the electrochemical method. In addition, the use of screen-printed sensors modified with CDs derived from natural resources for electrochemical detection of environmental pollutants is another important innovation of this work. Thereby, the novel NB electrochemical sensors based on CDs obtained from the HTC-EC integrated methodology, are certainly of high scientific value and may also add value to industrial citrus wastes.

## Results and Discussion

The aim of this work is the use of the liquid phase deriving from the HTC treatment of OPW, generally considered a non-exploitable waste.[12] Based on the results of our previous studies,[27] which evidenced that the optimal reaction conditions to obtain an aqueous phase rich in organic compounds, useful as raw materials for further EC treatment, the HTC experiments were performed at 180 °C for 60 minutes. The general chemical composition of the obtained liquid aqueous sample, hereafter named LHTC180-60, shows that the main compounds are furan derivatives, especially furfural (16.69 %) and 5-hydroxymethylfurfural (61.82 %), evidencing that, at low HTC temperatures (180 °C), one of the main compounds obtained in the liquid phase is 5-hydroxymethylfurfural (5-HMF).[27] The electrocatalytic conversion of 5-HMF has been widely demonstrated and this area of research is in the growth phase. Accordingly, the use of raw materials containing 5-HMF is of great importance for recovery, recycling, and circular chemistry. Based on our continuous efforts and experience in both biomass valorisation,[10] and the development of sustainable electrochemical methods,[28,29] an electrochemical process for producing carbon dots using the liquid phase from HTC, which is rich in 5-HMF, has been developed. In the field of carbon dots production from biomass waste, the use of the EC method represents a highly innovative application. The chosen electrochemical setup, consisting of an undivided cell employing two Pt spirals as electrodes and a potentiostat device, is cheap and easily available compared to other electro-synthesis techniques, and guarantees ease of operation and precise control over the amount of current flowing through the system. Under these conditions, the resulting mass yield (mY) of CDs was 37 % [see Eq. (2) in the Experimental Section]. Indeed, further increase of the applied potential from 8 V to 12 V results in low amounts of CDs performing with the same reaction time of 2.5 h. Figure S3 shows the effect of applied voltage (8–12 V) on mY of CDs.

CDs morphology was investigated by transmission electron microscopy (TEM). The representative images of CDs (Figure 1) confirmed the presence of monodispersed small circular nanoparticles and crystalline cores. Synthesized CDs exhibited an average diameter in the range of 1.47 nm to 6.67 nm.

The energy-dispersive X-ray spectroscopy (EDX) results (see Figure 2) indicate that the CDs contain mainly carbon, nitrogen, and oxygen, and no observable impurities were detected. EDX spectra of the CDs showed a high content of O due to many residual oxygen groups remaining on the surface.

Nitrogen can derive from other water-soluble components present in the starting biomass (orange peels). Moreover, the dynamic light scattering (DLS) measurement, reported in Figure 3a, confirmed the small size of the synthesized CDs and their dispersibility in water. Volume-weighted DLS measurements revealed a population centered at 10.1 nm, a value slightly higher than that obtained by TEM, and a polydispersity index (PDI) of 0.425, further confirming the tight particle size distribution.

Further confirmation of the electrical charges on the surface of nanoparticles and their colloidal stability was given by the zeta potential (Figure 3b), evaluated in the pH range of 6.0 to 8.0. Zeta-potential is a level of degree of electrostatic repulsion between contiguous similar charged particles in dispersed CDs.

The negative value of zeta potential indicates that the electrostatic forces are repulsive between the molecules. In the investigated pH range, the CDs surfaces were always negatively charged, consistent with the Fourier-transform infrared spectroscopy (FTIR) results (Figure 4b), suggesting the presence of

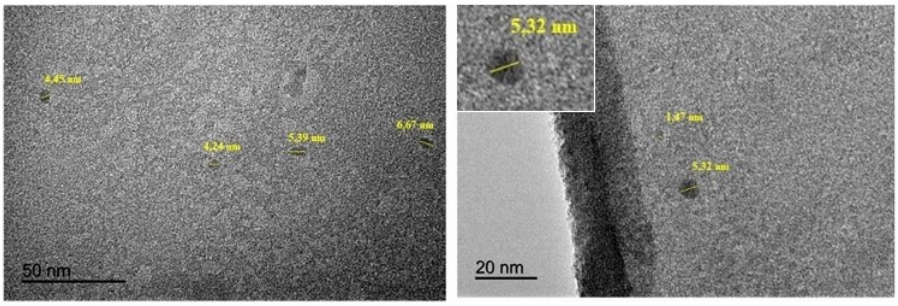


**Figure 1.** Representative TEM images of the obtained CDs.

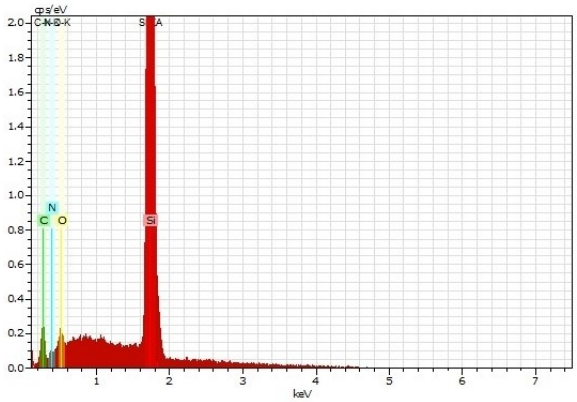


**Figure 2.** EDX spectrum of CDs.

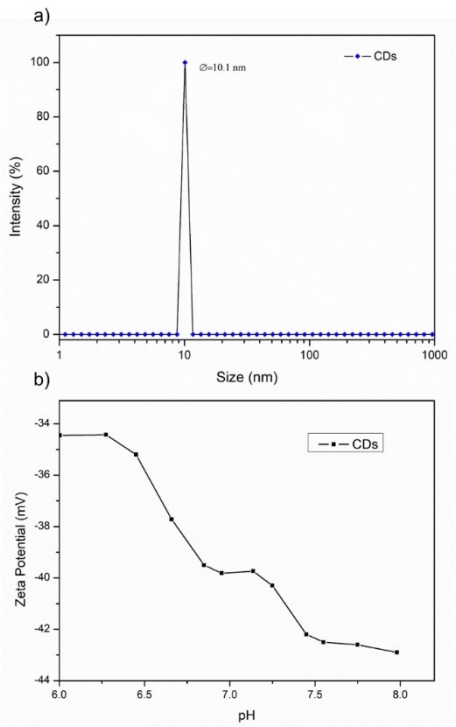


**Figure 3.** a) DLS size distribution and b) zeta potential at different pH values of CDs.

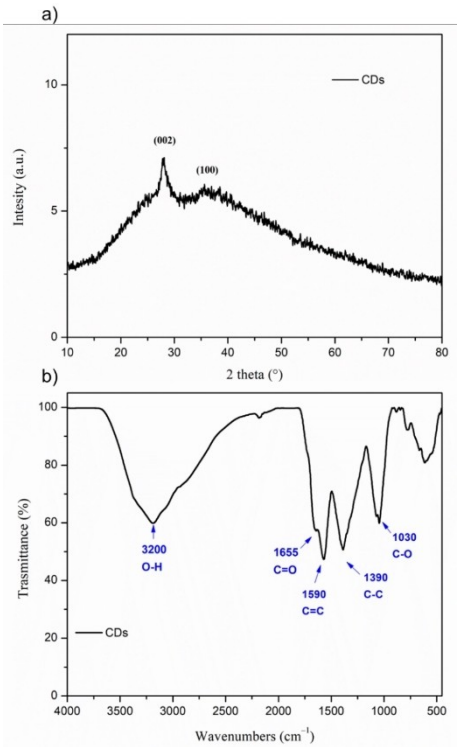


**Figure 4.** Compositional analysis of CDs: a) XRD spectrum; b) FTIR spectrum.

negatively charged hydroxyl (–OH) and carboxyl (–COOH) functional groups on their surface. The oxygen-rich and anionic functional groups present on CDs surfaces improved their hydrophilicity and stabilities in aqueous systems, which would be promising for sensing applications in aqueous media.

To acquire deeper information regarding the evolution of the microstructure and evidence about the surface groups present, CDs samples were investigated by X-ray diffraction spectroscopy (XRD) and FTIR (Figure 4a and b). The XRD diffraction spectrum (Figure 4a) shows a diffraction peak centered at $2\theta = 27°$ and $2\theta = 35°$ corresponding relatively to the (002) graphitic plane and the turbostratic structure of disordered carbon coming from the (100) plane of graphite.[30] The presence of different functional groups on CDs surface was confirmed by FTIR studies (Figure 4b). The FTIR spectrum of CDs shows the presence of oxygenated groups on the surface of the

nanomaterial. The strong, broad stretching band at 3200 $cm^{-1}$ in the IR spectrum, indicates the presence of an O–H alcohol group stretching by an intermolecular bonded functional group on prepared CDs while the peak at 1390 $cm^{-1}$ could be assigned to the O–H bending of the alcoholic groups.[31] Moreover, the adsorption bands at 1655 $cm^{-1}$ and 1590 $cm^{-1}$ correspond to the C=O vibrations and the C=C band respectively indicating the asymmetric stretching of aromatic rings, esters, amides or carboxylic groups, revealing the aromatization and decarboxylation reaction of the OPW during the hydrothermal process.[32]

As will be discussed later, the presence of these functional groups plays a crucial role in the selective interaction between the CDs and NB. As evidenced, the FTIR results indicate that the surface of CDs is rich of hydroxyl and carboxylic groups. As previously reported, it is probable that these hydrophilic groups may be due to the oxidation of the obtained carbon nanoparticles under electrochemical oxidation.

An electrochemical study of the CDs deposited on the SPCE platform (CDs/SPCE) was first performed. The study of Nyquist diagrams in electrical impedance spectroscopy (EIS) analysis shows the transfer capacity of the electron on the bare and modified sensor. The analysis was conducted in the presence of 10 mM $[Fe(CN)_6]^{3-/4-}$ and 0.1 M KCl, in the frequency range from 0.1 Hz to 105 Hz (amplitude 5 mV) and with an applied potential of 0.25 V. The size of the semicircle that can be observed at high frequencies indicates the resistance of the sensor to the charge transfer that takes place on its surface while the linear portion is attributed to the diffusion process that takes place on the sensor and can be observed at low frequencies.[33] Figure 5a shows the results obtained. The sensor modified with the CDs shows a very small semicircle diameter in the Nyquist plots (as reported in the inset in Figure 5a) compared to the bare SPCE. This indicates the ability of the new sensor functionalized with CDs to promote the transfer of electrons by improving the ability to start redox processes necessary for the detection of NB. Figure 5b shows the modeling of electrical equivalent circuit obtained from the collected data, which combines four components: the electrolytic resistance between the working and reference electrodes ($R_s$), the double layer capacitance (CPE), the charge transfer resistance ($R_p$) and the Warburg impedance ($W$).

The modified sensor CDs/SPCE has also been characterized through cyclic voltammetry (CV) analysis using 10 mM $K_3[Fe(CN)_6]$ solution with a scanning speed of 50 mV $s^{-1}$ (Figure 6). The recorded electrochemical behaviour shows a modified sensor higher peak current than the bare (202.56 μA versus 112.67 μA respectively) and a peak-to-peak separation ($\Delta E_p$) lower in CDs/SPCE than SPCE with 120 mV and 230 mV respectively. All this confirms the great ability of the modified sensor to promote the oxidation/reduction reaction by increasing the charge transfer compared to the bare, demonstrating better sensitivity.

The scan rate was obtained between 10 to 400 mV $s^{-1}$ studying the oxidation/reduction phenomenon affected on the sensor surface. The results shown in Figure 7a demonstrate an increase in oxidation peak and a shift in work potential with increasing scanning speed. Relating the maximum current peak to the square root of the scanning speed shows a linear trend (Figure 7b) which proves the capability of the CDs/SPCE sensor to promote the electrochemical process under diffusion control. The standard deviation (sd) was calculated on three repetitions for each measurement, resulting equal/less than 3 (Figure S4). The effective electrochemical active surface area of the prepared electrode was also determined from these data based on the Randles-Ševčik equation [Eq. (1)]. The effective electrochemical active surface area of CDs/SPCE was about 55% more compared to the bare. The formula was employed to determine the active surface area of the SPCE and CDs/SPCE using ferro/ferrocyanide as the redox probe.[34]

$$I_p = \pm 0.4463nFAC\sqrt{\frac{nFvD}{RT}} \quad (1)$$

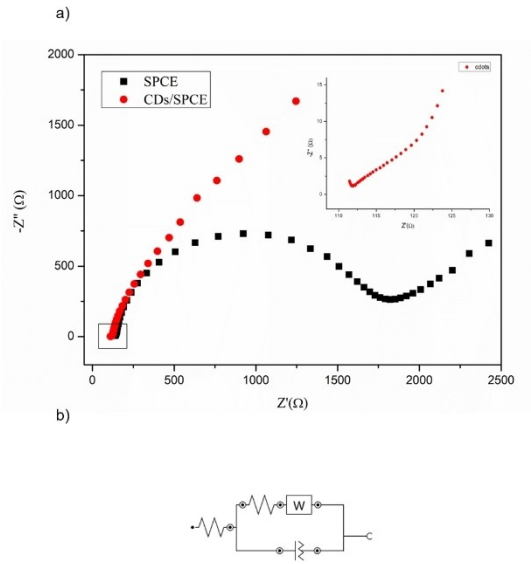


**Figure 5.** a) EIS of SPCE and CDs/SPCE in a solution containing 10 mM $[Fe(CN)_6]^{3-/4-}$ and 0.1 M KCl with a frequency range from 0.1 Hz to 105 Hz; amplitude 5 mV; b) electrical equivalent circuit.

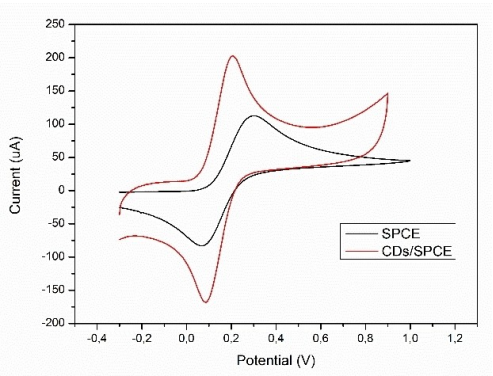


**Figure 6.** Cyclic voltammogram of SPCE and CDs/SPCE in presence of 10 mM $K_3[Fe(CN)_6]$ at a scan rate of 50 mV $s^{-1}$, in the potential range from −0.3 V to 0.9 V.

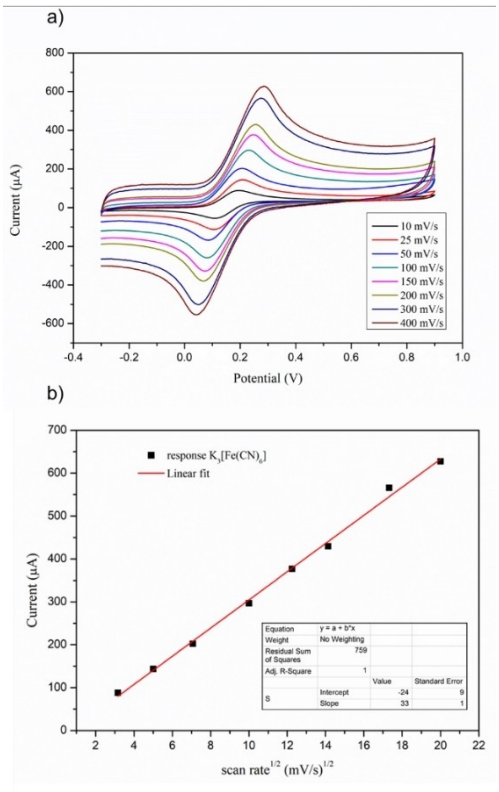


**Figure 7.** a) Cyclic voltammogram of CDs/SPCE in presence of 10 mM $K_3[Fe(CN)_6]$ at different scan rates between 10 and 400 mV $s^{-1}$ in 0.01 M PBs (pH 7.4), potential range −0.3 to 0.9 V; b) plot of $I_p$ vs $v^{1/2}$, sd ≤ 3 (see Figure S4).

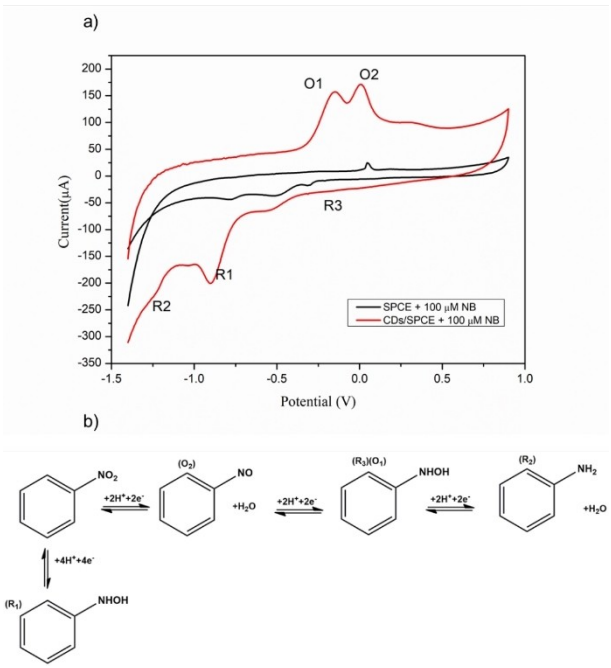


**Figure 8.** a) Electrochemical behavior of SPCE and CDs/SPCE with 100 μM NB in 0.01 M PBS at a scan rate of 50 mV $s^{-1}$ from −1.4 to 0.9 V potential window; b) chemical transformations of NB.

Where $I_p$ is the voltammetric current [A] using the forward peak of the electrochemical process, $n$ is the number of electrons transferred in the electrochemical reaction ($n = 1$), $F$ is the Faraday constant ($F = 96485.3365$ C $mol^{-1}$), $A$ is the electrode surface area [$cm^2$], $C$ is the concentration of the redox probe ($C = 10$ mM), $v$ is the applied voltammetric scan rate ($v = 0.05$ V $s^{-1}$), $D$ is the analytic diffusion coefficient ($D = 7.6 \times 10^{-6}$ $cm^2$ $s^{-1}$), $R$ is the universal gas constant ($R = 8.314$ J $mol^{-1}$), $T$ is the Kelvin temperature ($T = 298.15$ K).

CV of the SPCE and CDs/SPCE was performed in the potential range of −1.4 to 0.9 V in 0.01 M phosphate buffer solution (PBS) at pH 7.4. In the absence of NB, no faradaic peak was observed (Figure S5). The modified sensor exhibits a larger CV cycle than the SPCE one. This result indicates that the presence of CDs increases the active surface area of the electrode by increasing the available active sites. Further, in the presence of NB, CDs/SPCE sensor shows two very intense oxidation peaks (O1 and O2) at −0.15 and 0.01 V, and three reduction peaks (R1, R2 and R3) at −1.23 V, −0.9 V and −0.31 V respectively (Figure 8a). Literature data show that R1 peak is due to the irreversible reduction of NB to phenylhydroxylamine with subsequent reversible oxidation to nitrous benzene and reduction again to phenylhydroxylamine.[35,36] Therefore, the R1 peak observed with CDs/SPCE cycle is generated by the four-electron reduction of NB to phenylhydroxylamine, and then the phenylhydroxylamine continued to reduce to aniline through a two-electron process, namely the R2 peak. In the forward cycle, the phenylhydroxylamine produced through the reduction of NB was oxidized to nitrous benzene. Then, the produced nitrous benzene was reduced to phenylhydroxylamine, generating the R3 peak.[37] Therefore, is demonstrated that R1 and R3 reduction peaks are a redox couple of nitrous benzene and phenylhydroxylamine and the R2 reduction peak could be due to the direct formation of aniline from nitrobenzene.[38] Based on these data, it is possible to speculate that the oxidation peaks observed in this work may result not only from the reversible oxidation-reduction reaction of hydroxylamine to nitrous benzene but also from the oxidation of aniline formed during the redox process, as summarized in Figure 8b.

Figure 9a reports the linear sweep voltammetry (LSV) curves obtained at the different scan rate investigated, showing an increase in oxidation peak and a slight shift in potential with increasing scanning rate. Relating the maximum current peak ($I_{pa}$) to the scan rate shows a linear trend (Figure 9b) with an $R^2$ of 0.997. The sd was calculated on three repetitions for each measurement, resulting equal/less than 1.6 (Figure S7).

The effect of pH (Figure 10) on the reduction of NB (100 μM) was investigated by using standard buffer solution in PBS (0.01 M) in the range between 2.3 to 13.0 at a scan rate of 50 mV $s^{-1}$. The sensor response was enhanced as the pH increased from 2.3 to 7.4, but it decreased at pH values greater than 8.0. The corresponding curves obtained by differential pulse voltammetry (DPV) at different pH values showed that the reduction of the NB has improved at pH = 7.4. As reported in the literature,[36,38] the increase in reduction peak current at neutral pH is attributed to the influence of the hydrogen ion on

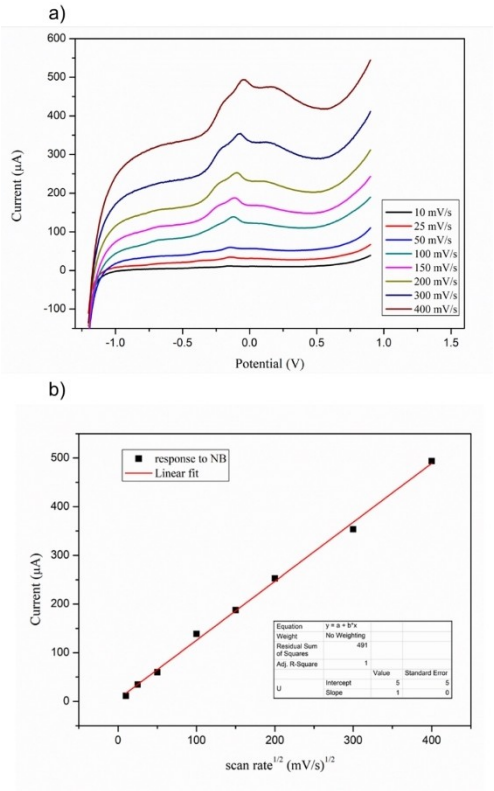


**Figure 9.** a) Linear sweep voltammogram of CDs/SPCE with 100 μM NB at different scan rates in 0.01 M PBs (pH 7.4); b) plot of $I_p$ vs $v^{1/2}$, sd ≤ 1.6 (Figure S7).

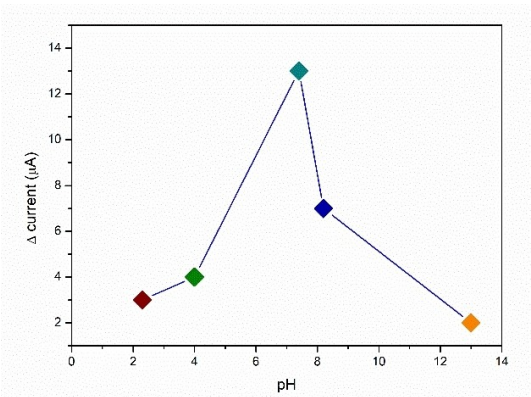


**Figure 10.** The pH effect on the reduction of NB.

the reduction of NB. Thus, the value of 7.4 was chosen as the optimum pH for further experiments.

The electroanalytical performances of the CDs/SPCE sensor were preliminarily assessed by studying its behavior for successive NB additions. NB is a compound rich in π-electrons and therefore interacts with CDs through the π–π interaction. Furthermore, the presence of weak bonds (such as hydrogen bonds) stabilizes the interaction between the CDs and the $NO_2$ group of the NB. As discussed in the characterization section, the presence of aromatic rings substituted by carboxyl and amide groups leads to interactions with nitrobenzene with a donor-acceptor electron transfer mechanism involving the $NO_2$ group. These interactions would attract more NB molecules onto the electrode surface and therefore the amplitude of the signal referred to the reduction is greater on the modified electrode than on the bare one. Furthermore, recent studies have shown that the pore structure and the small size of CDs (~less than 10 nm) promote interaction as they increase the contact surface area, showing higher detection activity.[38,40]

From the CV analysis, there is an increase in peak current as the NB concentration increases for the two oxidation peaks (O1 and O2) and the reduction peak (R1) (Figure S6a). However, at low concentrations of NB, only one oxidation peak can be observed due to the formation of nitrous benzene. An increase in the NB concentration generates a signal shift to more positive potentials and, by 10 μM, highlights the presence of the second oxidation peak. For the reasons explained, only the O2 oxidation peak, relating $I_{pa}$ to NB concentration, was considered. Two linear trends can be seen, one at low concentrations (0.1 to 0.6 μM) and another linear trend for concentrations between 10 and 100 μM (Figure S6b). The sensitivity of the sensor for NB is 768.54 μA μM$^{-1}$ cm$^{-2}$ for concentrations between 0–0.6 μM, while for concentrations between 10–100 μM the sensitivity is 4.86 μA μM$^{-1}$ cm$^{-2}$. The sensor denotes high sensitivity at low concentrations that decreases at concentrations above 10 μM most likely due to saturation of the active sites that promote the oxidation-reduction reaction. DPV test was carried out at different NB concentrations (Figure 11a) analyzing the reduction peak R1 because it appears to be the most sensitive in detecting changes in NB concentrations. To calculate the sensitivity and limit of detection (LOD) to NB of the CDs/SPCE sensor and obtain its calibration curve, NB additions were made in the range of 0.1 μM and 2 mM in 0.01 M buffer (PBS) solution at pH 7.4. The reduction current ($I_p$) showed a greater linear decrease with the change in NB concentration in CDs/SPCE (Figure 11b). The sensitivity was found to be 9.36 μA μM$^{-1}$ cm$^{-2}$ and the calculated LOD is 13 nM. LOD is the limit of detection and it represents the lowest concentration of the analyte that can be detected. It was calculated according to the IUPAC definition: 3.3 standard error/slope.[39,40] To determine the selectivity of the sensor, DPV tests were performed at a fixed concentration (100 μM) of different inorganic and organic pollutants. All measurements were made in 0.01 M PBS at pH 7.4 with a scan rate of 50 mV s$^{-1}$. The tested interfering substances are phenyl pyruvic acid, toluene, aniline, heavy metals (Cd, Pb, and Ni), nitrates, K, Cl, $NH_4Br$, picric acid and p-nitrotoluene. The addition of these compounds did not result in any change in the intensity of the detected current in the presence of 100 μM of NB, and therefore the modified sensor exhibited high selectivity over the reference analyte (Figure S8). The selective response to NB may further confirm that a response to this analyte is due to the bonds with the functional groups of the CDs and to the entrapment of the analyte's pores in the molecular cavities, which, according to a recent study, allows stronger interactions between NB and the structure of CDs framework.[41]

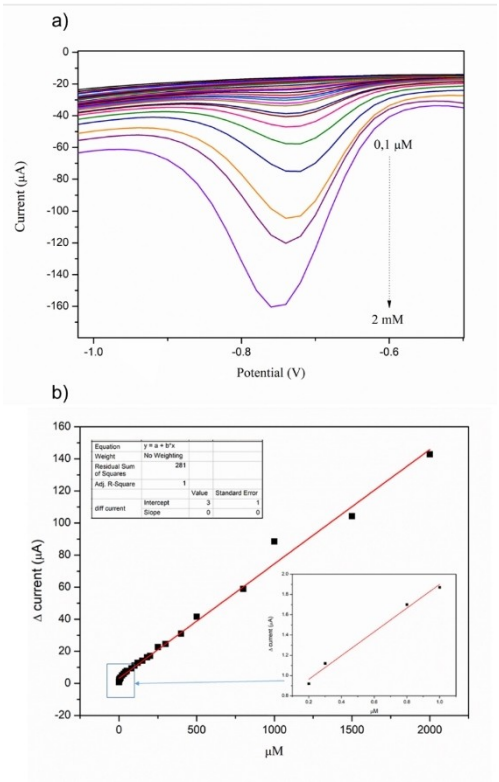


**Figure 11.** a) DPV of CDs/SPCE in 0.01 M PBS electrolyte and at different concentrations (0.1–2000 μM) of NB; b) calibration graphs for peak reduction currents, sd ≤ 2.

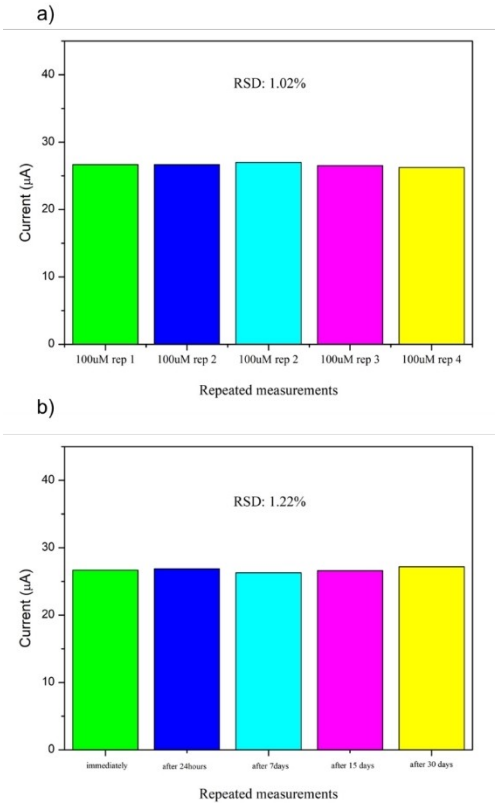


**Figure 12.** a) Repeatability test of CDs/SPCE performed by DPV in 0.01 M PBS electrolyte with 100 μM of NB; b) stability test of CDs/SPCE performed by DPV in 0.01 M PBS electrolyte with 100 μM of NB.

Furthermore, this selective behavior, can be attributed to the fact that under optimized electrochemical conditions, the NB reduction current is significantly greater than the similar molecules and therefore the modified sensor is able to detect the analyte selectively. Five tests were performed to check the repeatability and stability of the sensor by comparing the response of the sensor to the addition of NB in solution at the final concentration of 100 μM. The tests were carried out by monitoring the repeatability of the modified sensor during the analysis and over time. Figure 12a shows the results obtained after five repeated measurements. The average standard deviation (RSD) of the reduction peak determined by DPV was 1.02%, which shows that the modified electrochemical sensor has good repeatability. To verify the stability of the modified electrochemical sensor, it was tested for the detection of NB at the same concentration during different times: measurements were made after 24 hours and after 7, 15 and 30 days. Figure 12b showed satisfactory stability with an RSD of 1.22%. To investigate the application of the CDs/SPCE in real samples, DPV was performed to detect the NB in wastewater collected by industry in Milazzo (Sicily, Italy). No voltammetric signal was noticed for the wastewater sample, indicating that NB was absent in the sample. Different concentrations of NB were added to the real sample after dilution with 0.01 M PBS (wastewater: PBS ratio 1:9) using standard addition methodology to investigate the spiked recovery rate. Table 1 shows the percentage recovery of NB in a real sample performed by CDs/SPCE and compares it with literature data, highlighting that the obtained result exhibits similar or higher behavior. Therefore, the technology proposed in this study is satisfactory and has great prospects also for the practical analysis of NB in wastewater.

**Table 1.** Recovery values for NB detection in water real samples.

| Real sample | Recovery [%] | Sensitivity [μA $\mu M^{-1} cm^{-2}$] | LOD [nM] | Ref. |
|---|---|---|---|---|
| Wastewater | 93 | 1.27 | 150 | [35] |
| Wastewater | 99.35 | – | 10 | [36] |
| Lake water | 102.26 | 0.35 | 86 | [42] |
| Tap water | 99.7 | – | 7.3 | [43] |
| River water | 105 | – | 9 | [44] |
| Tap water | 101.36 | – | 1.56 | [45] |
| Lake water | 99.54 | – | 1.56 | [45] |
| Wastewater | 98 | 9.36 | 13 | Present work |

## Conclusion

To sum up, the CDs were synthesized starting from a green source, deriving from the hydrothermal carbonization treatment of orange peel waste generally considered a non-exploitable waste, by a bottom-up electrochemical synthesis, and then used to create an excellent electrochemical sensor for the detection of NB. OPW is a useful and economical raw material,

but it is very abundant and requires careful disposal. In this work, a new synthetic approach was pursued through the electrochemical treatment of the liquid phase obtained by HTC of OPW. This liquid fraction, which is still rich in small organic molecules, was valorized instead of the solid carbonaceous residue mainly used in the synthesis of carbonaceous nanomaterials. The synthesized CDs exhibited interesting physicochemical and optical properties, allowing their use as an electrochemical sensor. The sensor showed excellent redox activity for the detection of NB with a linear response range of 0.1–2000 μM and a detection limit of 0.013 μM. Moreover, the sensor exhibited satisfactory stability, high repeatability, and high selectivity for the determination of NB in the presence of interfering compounds. The sensing performance of the modified sensor was investigated in a real sample (wastewater), and the recoveries were 98%, indicating that the technique proposed in this study can be very effective in practical analysis in the environment field and could be used as a new device for the rapid determination of NB in the environmental matrix.

## Experimental Section

### Materials

All reagents used in this paper, were extra pure analytical grade and were purchased from Sigma-Aldrich. Ultrapure water (18.2 MΩ cm$^{-1}$) from a Milli-Q ultrapure system was used in this study.

### Electrochemical synthesis of CDs

The HTC experiments were performed following the procedure previously reported by our research group.[10] Based on the results obtained in the previous work,[27] the residence time, after reaching the reaction temperature, was set at 60 minutes, at a stirring speed of 750 rpm. Then, the solid and liquid products were separated by vacuum filtration, with a Buchner funnel and filter paper. The obtained liquid aqueous sample, hereafter named LHTC180-60, was employed as a raw material for the subsequent electrochemical bottom-up procedure. In a typical electrochemical synthesis of CDs, a solution 1 : 1 (*V/V*) of LHTC180-60 (0.121 g mL$^{-1}$) and $NH_3$ 30% was put in a glass sample vial. Two Pt wire spirals used as both cathode and anode electrodes (apparent area 1.0 cm$^2$) were immersed into the alkaline solution (see Figure S1 in Supporting Information for details about the experimental apparatus). A direct current stabilized power supply (Instrument Kert KAT4VD 1-30VDC 4A) was used to apply a static potential (8–12 V) between the two electrodes and the treatment was carried out at room temperature (25 °C) for 2.5 h. The obtained dark brown aqueous solution was centrifuged in order to remove large or aggregated big particles and to separate the dark solid from the supernatant. To further remove the matrix, the material was washed with ethanol and centrifuged three more times. Finally, pure, dark brown powder CDs were obtained after complete evaporation of the solvent. The mY of CDs was calculated using the following equation [Eq. (2)]:

$$\mathrm{mY[wt\,\%]} = \frac{m_{\mathrm{CDs}}[\mathrm{g}]}{m_{\mathrm{feedstock}}[\mathrm{g}]} \times 100\,\% \quad (2)$$

where $m_{CDs}$ is the mass of CDs, and $m_{feedstock}$ is the dry mass of OPW.

### Characterization of LHTC180-60 solution and CDs

Products in the aqueous liquid phase, as obtained after the separation of the solid carbonaceous fraction, were quantified by HPLC and GC–MS analysis, as previously reported.[27] Compound identification was performed by comparison with spectra obtained from the US National Institute of Standards and Technology (NIST) mass spectral library. The morphology and the particle sizes were investigated by TEM which was recorded on a JEOL JEM 1400 instrument with a lattice resolution of ca. 0.4 nm at 80 kV. TEM grids were prepared by depositing a drop of the synthesized CDs solution onto a carbon-coated copper grid and letting it dry for 30 minutes at room temperature before starting the analysis. A high-resolution Auriga-Zeiss (Jena, Germany) field emission scanning electron microscope (FE-SEM) operating at 10 kV and EDX system equipped with Bruker Quantax detector were used for the chemical composition characterization. The particle size and zeta potential measurements were performed by DLS analyses using the Zetasizer 3000 instrument (Malvern), equipped with a 632 nm HeNe laser, operating at a 173-degree detector angle. FTIR spectra were obtained by using a Spectrum Two FTIR Spectrometer (PerkinElmer Inc.) equipped with a universal ATR sampling accessory. The spectra were registered at room temperature in the range from 4000 to 500 cm$^{-1}$ with a scanning speed of 2 mm s$^{-1}$, resolution of 4.0 cm$^{-1}$ and accumulation of 30, without any preliminary treatment. The crystalline structure of synthesized materials was investigated using XRD by means of a Bruker D8 Advance A25 X-ray diffractometer, operating at 40 kV and in the range 10–80° (2$\theta$), with an increasing rate of 0.01° s$^{-1}$ using the CuKa1 radiation and the recorded diffractograms were developed via OriginPro 2019 software.

### Modified electrode fabrication

SPCEs mod C110, were purchased from DropSens (Methrom). The sensor platform consists of a ceramic substrate with a length of about 3.5 cm and a diameter of 4.0 mm, on which the electrochemical cell consists of three components: the carbon working electrode, the silver pseudo reference electrode, and the carbon counter electrode. A picture of the bare SPCE platform and its specifications is reported in Figure S2. The modified CDs/SPCE sensors were fabricated by dispersing, using ultrasound, 1 mg of CDs in 1 mL of distilled water. Then 10 μL of each suspension was drop cast on the surface of the working carbon electrode. After any dropping, the electrode was permitted to dry before the successive dropping. The sensors thus modified were allowed to dry at room temperature overnight.

### Electrochemical measurements

CV, LSV and DPV experiments were performed by using DropSens μStat 400 Potentiostat empowered by Dropview 8400 software for data acquisition. EIS analyses were performed using a potentiostat Galvanostat by Metrohom autolab in a solution containing 10 mM $[Fe(CN)_6]^{3-/4-}$ and 0.1 M KCl with a frequency range from 0.1 Hz to 105 Hz and amplitude of 5 mV. The sensors were characterized by CV and LSV. These latter was carried out in aerated 0.01 M PBS electrolyte at different scan rate in the potential range between −1.2 V to 0.9 V; CV tests were carried out at a scan rate of 50 mV s$^{-1}$ in the potential range from −0.8 to 0.9 V in a solution containing 10 mM $[Fe(CN)_6]^{3-/4-}$ and 0.1 M KCl and from −1.4 to 0.9 V in 0.01 M PBS by varying the concentration of the investigated analyte in order to study the redox behaviour of NB. DPV technique was carried out in 0.01 PBS electrolyte in a potential range between −1.2 and −0.5 V by applying amplitude potential pulse of 0.09 V for 200 ms, with a potential step of 0.02 V and scan rate of 50 mV s$^{-1}$. The calibration curves were obtained by plotting the

faradaic current vs the analyte's concentration. The sensitivity was computed as the slope of the calibration curve.

## Acknowledgments

*The authors acknowledge Sapienza University of Rome for financial support, and Center on Nanotechnologies Applied to Engineering of Sapienza (CNIS).*

## Conflict of Interest

The authors declare no conflict of interest.

## Data Availability Statement

The data that support the findings of this study are available from the corresponding author upon reasonable request.

**Keywords:** carbon nanodots · electrochemical sensor · electrochemical bottom-up synthesis · waste valorization · nitrobenzene

[1] FAS-USDA -Foreign Agricultural Service-United States Department of Agriculture. Citrus: World Markets and Trade. Available online: https://apps.fas.usda.gov/psdonline/circulars/citrus.pdf (accessed on 25 October 2022).
[2] K. Rezzadori, S. Benedetti, E. R. Amante, *Food Bioprod. Process.* **2012**, *90*, 606–614.
[3] D. Iannazzo, Celesti, C. Espro, A. Ferlazzo, S. V. Giofrè, M. Scuderi, S. Scalese, B. Gabriele, R. Mancuso, I. Ziccarelli, G. Visallim, A. Di Pietro, *Pharmaceutica* **2022**, *14*, 2249.
[4] V. Bressi, A. Ferlazzo, D. Iannazzo, C. Espro, *Nanomaterials* **2021**, *11*,1120.
[5] D. Iannazzo, C. Celesti, C. Espro, *Biotechnol. J.* **2021**, *16*, 1900422.
[6] D. Qu, Z. Sun, *Mater. Chem. Front.* **2020**, *4*, 400–420.
[7] T. Len, V. Bressi, A. M. Balu, T. Kulik, O. Korchuganova, B. Palianytsia, C. Espro, R. Luque, *Green Chem.* **2022**, *24*, 7801–7817.
[8] C. I. Wang, W. C. Wu, A. P. Periasamy, H. T. Chang, *Green Chem.* **2014**, *16*, 2509–2514.
[9] Y. Hou, Q. Lu, J. Deng, H. Li, Y. Zhang, *Anal. Chim. Acta* **2015**, *866*, 69–74.
[10] C. Espro, A. Satira, F. Mauriello, Z. Anajafi, K. Moulaee, D. Iannazzo, G. Neri, *Sens. Actuators B* **2021**, *341*,130016.
[11] V. Bressi, A. M. Balu, D. Iannazzo, C. Espro, *Curr. Opin. Green Sustain. Chem.* **2023**, *40*, 100742.
[12] E. Erdogan, B. Atila, J. Mumme, M. T. Reza, A. Toptas, M. Elibol, J. Yanik, *Bioresour. Technol.* **2015**, *196*, 35–42.
[13] F. Niu, Y. Xu, J. Liu, Z. Song, M. Liu, J. Liu, *Electrochim. Acta* **2017**, *236*, 239–251.
[14] P. R. Yaashikaa, P. Senthil Kumar, S. Varjani, *Bioresour. Technol.* **2022**, *343*, 126126.
[15] F. W. S. Lucas, R. G. Grim, S. A. Tacey, C. A. Downes, J. Hasse, A. M. Roman, C. A. Farberow, J. A. Schaidle, A. Holewinski, *ACS Energy Lett.* **2021**, *6*, 1205–1270.
[16] T. Xiao, J. Huang, D. Wang, T. Meng, X. Yang, *Talanta* **2020**, *206*, 120210.
[17] P. K. Arora, H. Bae, *J. Chem.* **2014**, *13* (31), 265140.
[18] T. Carreon, M. J. Hein, K. W. Hanley, S. M. Viet, A. M. Ruder, *Occup. Environ. Med.* **2014**, *71*, 175–182.
[19] A. Yousaf, N. Xu, A. M. Arif, J. Zhou, C. Y. Sun, X. L. Wang, Z. M. Su, *Dyes Pigm.* **2019**, *163*, 159–167.
[20] J. P. Cheng, T. Hu, W. J. Li, Z. D. Chang, C. Y. Sun, *J. Solid State Chem.* **2020**, *282*, 121125.
[21] R. Gupta, P. K. Rastogi, V. Ganesan, D. K. Yadav, P. K. Sonkar, *Sens. Actuators B* **2017**, *239*, 970–978.
[22] Z. Cheng, W. Mo, Y. Chen, H. Liu, X. Li, H. Ma, S. T. Zhang, *Microchem. J.* **2022**, *172*, 106896.
[23] S. J. Lee, J. Theerthagiri, M. Y. Choi, *Chem. Eng. J.* **2022**, *427*, 130970.
[24] J. Theerthagiri, S. J. Lee, K. Karuppasamy, J. Park, Y. Yu, M. L. Aruna Kumari, S. Chandrasekaran, H.-S. Kim, M. Y. Choi, *J. Hazard. Mater.* **2021**, *420*, 126648.
[25] J. Barton, M. B. G. García, D. H. Santos, P. Fanjul-Bolado, A. Ribotti, M. McCaul, D. Diamond, P. Magni, *Microchim. Acta* **2016**, *183*, 503–517.
[26] Z. Taleat, A. Khoshroo, M. Mazloum-Ardakani, *Microchim. Acta* **2014**,*181*, 865–891.
[27] A. Satira, E. Paone, V. Bressi, D. Iannazzo, F. Marra, P. S. Calabrò, F. Mauriello, C. Espro, *Appl. Sci.* **2021**, *11*, 10983.
[28] F. Pandolfi, I. Chiarotto, L. Mattiello, D. Rocco, M. Feroci, *Synlett.* **2019**, *30*, 1215–1218.
[29] I. Chiarotto, L. Mattiello, F. Pandolfi, D. Rocco, M. Feroci, R. Petrucci, *ChemElectroChem* **2019**, *6*, 4511–4521.
[30] A. Mewada, S. Pandey, S. Shinde, N. Mishra, G. Oza, M. Thakur, M. Sharon, M. Sharon, *Mat. Sci. Eng. C* **2013**, *33*, 2914–2917.
[31] B. Majumdar, S. Mandani, T. Bhattacharya, D. Sarma, T. K. Sarma, *J. Org. Chem.* **2017**, *82*, 2097–2106.
[32] A. Singh, G. Singh, S. Sharma, N. Kaur, N. Singh, *ChemistrySelect* **2022**, *7*, e2022009.
[33] S. Sarat, N. Sammes, A. Smirnova, *J. Power Sources* **2006**, *160*, 892–896.
[34] V. Bressi, Z. Akbari, M. Montazerozohori, A. Ferlazzo, D. Iannazzo, C. Espro, G. Neri, *Sensors* **2022**, *22*, 900.
[35] B. Thirumalraj, S. Palanisamy, S. M. Chen, K. Thangavelu, P. Periakaruppan, X. H. Liu, *J. Colloid Interface Sci.* **2016**, *475*, 154–160.
[36] T. Kokulnathan, A. Irudaya Jothi, S. Chen, G. Almutairi, F. Ahmed, N. Arshi, B. AlOtaibi, *J. Environ. Chem. Eng.* **2021**, *9*, 106310.
[37] Y. P. Li, H. B. Cao, C. M. Liu, Y. Zhang, *J. Hazard. Mater.* **2007**, *148*, 158–163.
[38] V. M. Kariuki, S. A. Fasih-Ahmad, F. J. Osonga, O. M. Sadik, *Analyst* **2016**, *141*, 2259–2269.
[39] A. D. IUPAC McNaught, A. Wilkinson, *Compendium of Chemical Terminology*, 2nd ed. (the "Gold Book"), Oxford **1997**.
[40] A. R. M. Rosli, F. Yusoff, S. H. Loh, H. M. Yusoff, M. M. Jamil, *J. Teknolog.* **2021**, *83*, 85–92.
[41] R. B. Lin, S. Y. Liu, J. W. Ye, X. L. Li, J. P. Zhang, *Ad. Sci.* **2016**, *3*, 500434.
[42] S. An, N. Shang, J. Zhang, A. Nsabimana, M. Su, S. Zhang, Y. Zhang, *Colloids Surf. A* **2022**, *653*, 130078.
[43] A. Ajitha, S. A. John, *New J. Chem.* **2022**, *46*, 6446–6452.
[44] O. J. Kingsford, J. Qian, D. Zhang, Y. Yi, G. Zhu, *Anal. Methods* **2018**, *10*, 5372–5379.
[45] C. Zhou, J. Xie, S. Zheng, Y. Chen, W. A. Gao, *Inorg. Chem. Commun.* **2022**, *143*, 109789.

Manuscript received: January 5, 2023
Revised manuscript received: February 22, 2023
Version of record online: ■■, ■■

# RESEARCH ARTICLE

**Not just waste**: An integrated approach based on linking thermal and electrochemical technologies is investigated for the valorisation of agro-industrial waste. The obtained carbon dots (CDs) are certain of high scientific value and may add more value to industrial citrus waste. The CDs exhibited interesting physico-chemical and optical properties, allowing their use as a voltammetric sensor.


*Dr. V. Bressi, Prof. I. Chiarotto*, Dr. A. Ferlazzo, Dr. C. Celesti, Dr. C. Michenzi, Dr. T. Len, Prof. D. Iannazzo, Prof. G. Neri, Prof. C. Espro**

1 – 10

**Voltammetric Sensor Based on Waste-Derived Carbon Nanodots for Enhanced Detection of Nitrobenzene**